Synthesis and characterization of N-guanidinium chitosan/silica ionic hybrids as templates for calcium phosphate mineralization

Ahmed Salama, Peter Hesemann

Synthesis and characterization of chitosan-N-guanidinium/silica ionic hybrids as templates for calcium phosphate mineralization

Ahmed Salama[1, 2,*] and Peter Hesemann[1]

[1]Institut Charles Gerhardt de Montpellier, UMR CNRS 5253 Université de Montpellier-CNRS-ENSCM, Place Eugène Bataillon, 34095 Montpellier Cedex 05, France

[2]Cellulose and Paper Department, National Research Centre, 33 Bohouth St., Dokki, Giza 12622, Egypt

E-mail: ahmed_nigm78@yahoo.com

Tel:+201008842629

Abstract

We report novel materials for calcium phosphate mineralization processes. These materials were synthesized via a three-step procedure starting from chitosan. In a first step, *N*-guanidinium-chitosan acetate was prepared via a direct guanylation reaction with cyanamide. This intermediate was then used as a cationic polymer substrate for attracting two functional anionic silica precursors, which subsequently allowed accessing new ionic hybrid materials *via* sol-gel chemistry. These *N*-guanidinium-chitosan acetate/silica hybrid materials containing either sulfonate or carboxylate groups were characterized using solid state ^{13}C NMR and ^{29}Si NMR and FT-IR spectroscopy. Finally, these two ionic hybrids were used as templates for *in-vitro* biomimetic calcium phosphate mineralization using simulated body fluid solution. We could show that the two ionic hybrids act as versatile templates for biomineralization, inducing the formation of hydroxyapatite, as proved from XRD, SEM, EDX, TEM and TGA. The current results suggest that the new ionic hybrid may be promising candidates for bone tissue engineering applications.

Keywords

Chitosan – Ionic hybrids – Biomimetic mineralization – Calcium phosphate

Graphical Abstract

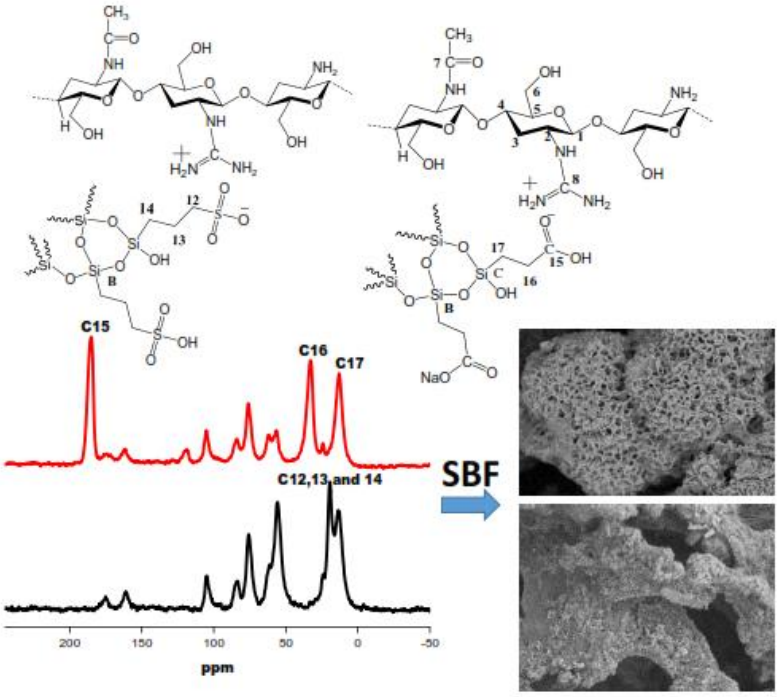

1. Introduction.

Calcium phosphate with controlled morphologies and hierarchical structure recently triggered extensive research in the area of biomaterials [1,2]. Organic matrix mediated biomineralization using templates such as collagen and amino acids were found to modulate efficiently calcium phosphate mineralization in living organisms [3]. Moreover, anionic non-collagenous proteins are reported to induce hydroxyapatite deposition within collagen fibers [4]. Due to the limitations and high cost of non-collagenous proteins, several attempts to mimic these proteins via the use anionic polymers like poly(acrylic acid) and poly(aspartic acid) were reported [5,6]. Recently, it was shown that functionalized polysaccharides with appropriate biocompatibility and biodegradability can exert a strong influence on the external morphology and crystalline structure of inorganic mineralization [1,7,8].

Chitosan, *i.e.* deacetylated chitin, is a linear polysaccharide composed of glucosamine and N-acetylglucosamine units linked by β (1–4) glycosidic bonds. Chitosan is among the most studied polysaccharides and can chemically be modified to obtain derivatives with improved biological properties. The presence of primary amine groups as well as primary and secondary hydroxyl groups allows its derivatization and the introduction of functional groups via covalent or ionic bonding with silica precursors [9–11]. Due to their biocompatibility, biodegrability, anti-bacterial activity and cellular compatibility, chitosan derivatives are promising candidates for applications in the biomedical field [12]. However, in the area of biomineralization, chitosan-based frameworks showed low efficiency for controlled nucleation and growth of inorganic materials, especially calcium phosphate, because of their smooth surface [13,14]. Only few studies have been reported which evaluate the potential of chitosan as template for controlling the biomineralization processes. For example, Wang et. al. prepared specific hierarchical structures from chitosan/calcium phosphate nanocomplexes through ionotropic gelation using tripolyphosphate as both cross linking agent and phosphate precursor. The porous texture of the prepared hybrid material results in a high efficiency in dye adsorption and enzymatic catalysis [15]. Another trial was carried out by using genipin as crosslinking reagent to access hydroxyapatite coated genipin-chitosan scaffolds. The results showed that the mineralized hydroxyapatite nanocrystals mechanically reinforce the produced materials. Moreover, the biomimetically synthesized hydroxyapatite influences the

cellular morphology and the cytoskeleton organization of rat bone marrow-derived mesenchymal stem cells [14].

The guanidinium moiety is an important active unit for many biological receptors especially those for RNA[16]. It can be found in many drugs with numerous therapeutic applications and biological activities such as antidiabetic [17] and broad-spectrum antimicrobial drugs [18]. Moreover, the guanidinium group can form ionic interaction with a wide range of anionic functional groups like carboxylate and phosphate as well as hydrogen bonding [19]. Several trials have been carried out to prepare guanidinium functionalized chitosan *via* the reaction between chitosan and arginine [20] or through direct guanylation between chitosan and cyanamide [10,11].

The sol-gel technique has been widely used to produce functional hybrid materials because it has allowed overcoming the difficulty of using the classical silica glass-based biomaterials for manipulating the internal microstructure of the matrix as well as avoiding high temperature [21]. A huge number of organic functional groups can be incorporated within silica matrices *via* the sol-gel process, ranging from active pharmaceutical ingredients to polysaccharides [22] and synthetic polymers [23] up to biological entities, like peptides [24], with the aim of providing enhanced functionality to the resulting biomaterials.

In this article, we report new chitosan/silica hybrid materials for calcium phosphate mineralization. Firstly, the guanylation of neat chitosan was carried out in acidic aqueous solution using scandium(III) triflate as a catalyst. Then, this cationic *N*-guanidinium chitosan acetate was treated with two anionic silica precursors to form new *N*-guanidinium chitosan/silica ionic hybrids via sol-gel chemistry. The formation of these supramolecular hybrids consisting of *N*-guanidinium chitosan acetate and hybrid silica result from a high affinity between these two components which is based on ionic interactions between the cationic guanidinium groups of chitosan and the anionic functions of the silica precursors. Finally, we investigated the activity of the two ionic hybrids toward calcium phosphate mineralization from simulated bidy fluid (SBF) solutions. This strategy towards three-dimensional ionic templates increases the density of functional groups that act as nucleation sites toward inorganic mineralization. The chemical composition, morphology, internal crystal structure and content of the biomimetically mineralized calcium phosphate was investigated as a

function of the quantity of sulfonate or carboxylate groups in intermediate ionic hybrids.

2. Materials and methods.

2.1. Materials

Medium molecular weight chitosan (degree of deacetylation, 75-85%), acetic acid, cyanamide, scandium(III) triflate were obtained from Sigma-Aldrich. Carboxyethylsilanetriol, sodium salt; 25% in water and 3-(trihydroxysilyl)-1-propansulfonic acid, 30-35% in water were supplied from ABCR GmbH. All chemicals were of analytical grade and used without further purification. All aqueous solutions were prepared using deionized water.

2.2. Syntheses

2.2.1. *N*-guanidinium chitosan acetate (GC). 10 ml of a 2% solution of chitosan in 2% acetic acid was mixed with 84 mg cyanamide (0.002 mol) and 30 mg (60 nmol) of scandium(III) triflate. The solution was stirred at 100°C for 48 h and the resulting mixture was precipitated and washed repeatedly with acetone. The guanuylated material **GC** was obtained as a white powder.

2.2.2. GC/silica containing sulfonic acid and carboxylate groups ionic hybrids (CGSS and CGSC). N-guanidinium chitosan/silica containing sulfonic and carboxylic acid ionic hybrid were synthesized in two steps. In the first step, to a solution of material **GC** (0.4 g) in 100 ml of deionized water 2 equivalents of 3-(trihydroxysilyl)-1-propanesulfonic acid or carboxyethylsilanetriol, sodium salt were added under vigorous stirring. Then, 0.02 M HCl solution (10 mL) was slowly added into the alkoxide solution and the mixture was heated at 60 °C for 48 h. Finally, the resulting white suspension was filtered. The precipitates of **CGSS** and **CGSC** were thoroughly washed with deionized water until neutral pH and finally washed with methanol followed by freeze-drying for 24 h.

2.3. Calcium phosphate biomineralization.

Biomimetic calcium phosphate mineralization was carried out as described in our previous study [25]. The ionic hybrids **CGSC** and **CGSS** were soaked in doubly

concentrated simulated body fluid (2 x SBF) to enhance the biomimetic calcium phosphate nucleation. The biomimetic mineralization process continued for 7 days after soaking the ionic hybrids in 100 mL 2 x SBF with continuous renewed every 24 h. The mineralized **CGSC** and **CGSS** hybrids were washed with water then dried in a freeze-drier.

2.4. Characterization methods.

2.4.1. FT-IR Spectroscopy. The attenuated total reflectance Fourier transform infrared (ATR-FTIR) spectra of materials were obtained using a Thermo Nicolet FT-IR Avatar 320 with a diamond crystal Spectra were recorded from 500 to 4000 cm^{-1}.

2.4.2. Solid state NMR spectroscopy. ^{29}Si-NMR spectra were recorded on a Varian VNMRS 400 MHz spectrometer using a two-channel probe with 3.2 mm ZrO_2 rotors. ^{13}C Cross Polarization Magic Angle Spinning (CP/MAS) was used to obtain a high signal-to-noise ratio with 5 ms contact time and 5 s recycling delay.

2.4.3. Thermogravimetric Analysis. TGA measurements were carried out with a NETZSCH STA 409 PC instrument. All materials were burned under air flux between 25 and 900 °C at a heating rate of 5°C/min.

2.4.4. SEM Analysis. The surface morphology of *N*-guanidinium chitosan and the *N*-guanidinium chitosan silica microhybrid was determined by using a Hitachi S-4800 scanning electron microscope.

3. Results and discussion

3.1. Methodology

In a first step, *N*-guanidinium chitosan acetate (**GC**) was synthesized through a direct guanylation reaction between chitosan and cyanamide in the presence of scandium (III) triflate as reported in our previous studies [10,11]. The two different anionic silica precursors, carboxyethylsilanetriol sodium salt and 3-(trihydroxysilyl)-1-propansulfonic acid, have been used to form **GC**-silica hybrid composites via a sol-gel reaction. Ionic interactions between **GC** and the silica precursors ensured high affinity between both components and led to the formation of *N*-guanidinium-chitosan acetate/silica containing sulfonate groups (**CGSS**) and *N*-guanidinium-chitosan acetate/silica containing carboxylate groups (**CGSC**). The bioactivity of the two hybrid materials was finally investigated toward biomimetic calcium phosphate mineralization, thus yielding the mineralized hybrid materials containing calcium phosphate **CGSS-CP** and **CGSC-CP**. All materials were characterized to monitor the chemical and morphological modifications induced by *i*) the sol-gel reaction and *ii*) the calcium phosphate mineralization process.

3.1. IR spectroscopic analyses

The FT-IR spectra of chitosan and *N*-guanidinium-chitosan together with those of the **CGSC** and **CGSS** ionic hybrids and mineralized hybrids are shown in figure 1. The spectra of chitosan and **CG** are virtually similar and show the same characteristic bands of the chitosan skeleton. The broad band at 3450 cm^{-1} can be attributed to NH, OH symmetric stretching vibration and inter- and intra-molecular hydrogen bonds of chitosan molecules. The weak band at 2921 cm^{-1} is ascribed to the C-H stretching vibrations of chitosan and the characteristic peaks at 1656 and 1580 cm^{-1} are due to the C=O stretching (amide I) and –NH stretching (amide II), respectively. However, the increase of the intensity of the adsorption band at 1630 cm^{-1} observed in the spectrum of **CG** suggests the presence of guanidinium moiety as shown in figure 1[10].

The spectrum of GC After the sol-gel reaction with the two silica hybrid precursors show strong absorption bands between 1100 and 1000 cm^{-1} which can be assigned to the siloxane networks (Si–O–Si) [26]. The presence of these typical silica peaks in the spectra of two ionic hybrids (**GCSS** and **GCSC**) confirms the formation of a silica

network around the *N*-guanidinium-chitosan acetate polymer chains. Furthermore, **GCSS** and **GCSC** ionic hybrids showed a broad band at 3200−3500 cm^{-1} that can be assigned to the silanol groups, localized on the surface of the silica hybrid material due to the incomplete condensation reaction under acid-catalyzed conditions. This incomplete condensation in the silica is beneficial for improving the compatibility between silica and *N*-guanidinium-chitosan acetate through hydrogen bonding. After calcium phosphate mineralization by immersing the two ionic hybrids in simulated body fluid (SBF) solution, the two mineralized hybrids exhibited the characteristic bands of phosphate group vibration modes. The peaks at 1033 and 1180 cm^{-1} (P-O ν_3 mode), 569 cm^{-1} (P-O ν_4 mode), and 904 cm^{-1} (P-O ν_1 mode) are assigned to **CGSC-CP**. In addition, nearly the same vibration modes were also found in the spectrum of the sulfonate sample **CGSS-CP**. These results confirm that a mineralization process took place.

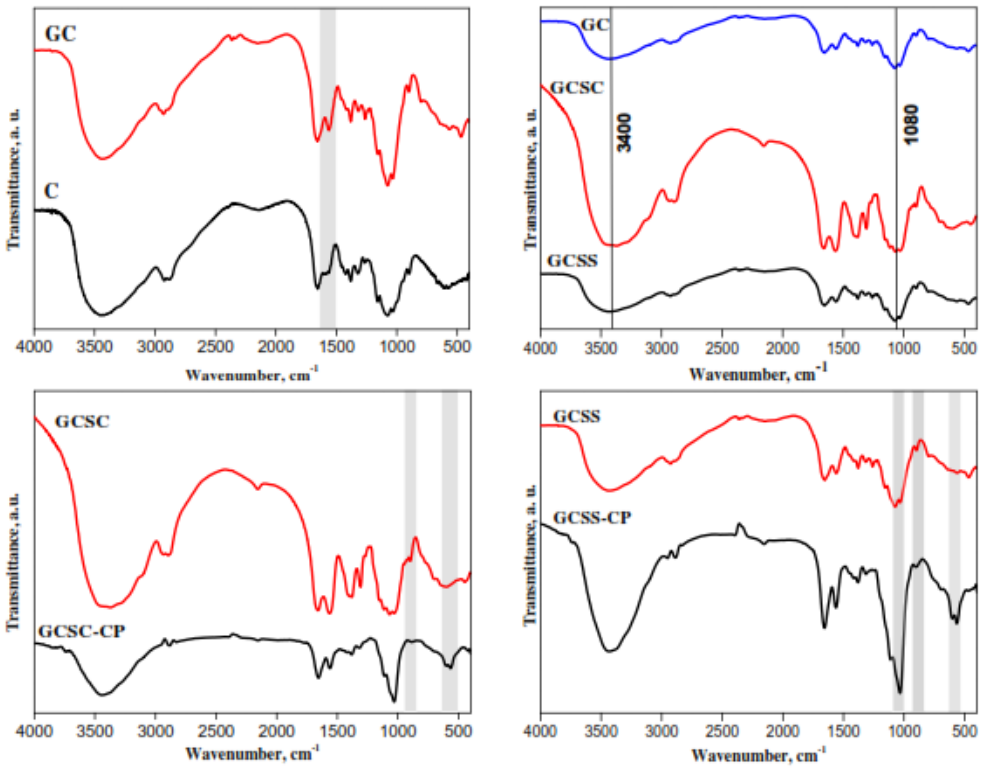

Figure 1: FT-IR spectra of chitosan (C), **GC**, **GCSC**, **GCSS**, **GCSC-CP** and **GCSS-CP**.

3.2. Solid state NMR spectroscopy

The solid state NMR spectroscopic analysis allows monitoring the chemical modification of the materials. Here, we can get information about the chemical modification of chitosan *via* guanylation, resulting in the formation of the material **GC**, and, in a second time, the formation of the chitosan/silica hybrid composites **CGSC** and **CGSS**.

The spectra of neat chitosan and **GC** are given in the supporting information. As already reported in our previeous work [10], the appearance of a signal at a chemical shift of δ=160 ppm in the ^{13}C CP-MAS spectrum of **GC** reflects the presence of the newly formed guanidinium groups. Furthermore, a shoulder at around 180 ppm can be attributed to acetate counter anions, as the guanylation reaction was performed in the presence of acetic acid. In this way, ^{13}C CP-MAS solid state NMR spectroscopy gives clear evidence for the formation of the chitosan supported guanidinium acetate groups.

The ^{13}C CP-MAS solid state NMR spectra of the **CGSC** and **CGSS** ionic hybrids are given in figure 2. In the spectrum of **CGSC, new signals in the range of** 13-32 ppm and at 185 ppm indicate the presence of the organosilylated carboxylate precursor and can be attributed to the carbon centers of the ethyl chain (C15/C16) and the carboxylate groups (C14), respectively. On the other side, the ^{13}C CP-MAS solid state NMR spectra of the sulfonate ionic hybrid **CGSS** shows new signals resonances in the range of 13-19 ppm characteristic for the propyl chain of the silylated sulfonate precursor (C12/C13/C14). Finally, the disappearance of the signal at around 180 ppm reflects the substitution of acetate anions via anion exchange involving the silylated carboxylate or sulfonate compounds.

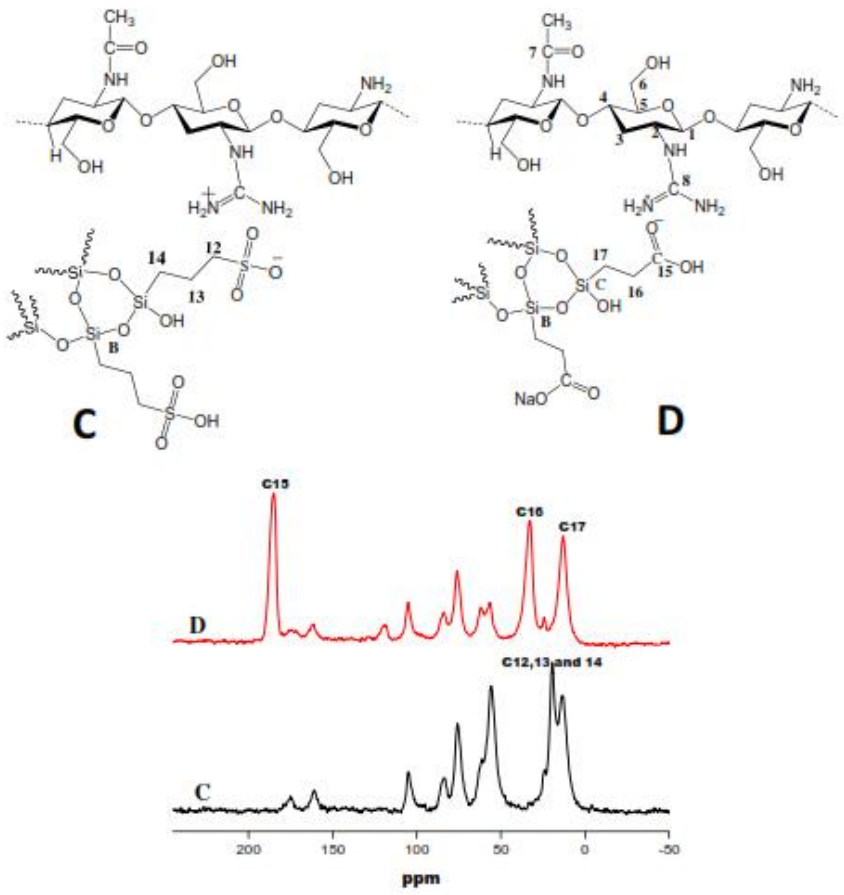

Figure 2. ^{13}C NMR of **CGSS** (C) and **CGSC** (D)

On the other side, ^{29}Si One solid state NMR spectroscopy allows getting detailed information about the predominant environment of the silicon centers in the silica hybrid matrix. The ^{29}Si One Pulse (OP)-MAS solid state NMR spectra of **GCSS** and **GCSC** are given in figure 3. Both spectra show intense signals at -67.5 ppm together with peaks of lower intensity at -58 ppm. These results suggest that the silicon nuclei are mostly present as R<u>Si</u>$(OSi)_3$-environment, but that significant amounts of R<u>Si</u>$(OSi)_2(OH)_1$-species are also present. Surprisingly, the weak resonances of Q^n species in GCSS hybrid at -100.3 and -109.7 ppm indicate the presence of Si $(O–Si)_n$ $(OH)_{4-n}$ silicon centers which may originate from a small amount of Si-R cleavage during the hydrolysis-polycondensation procedure.

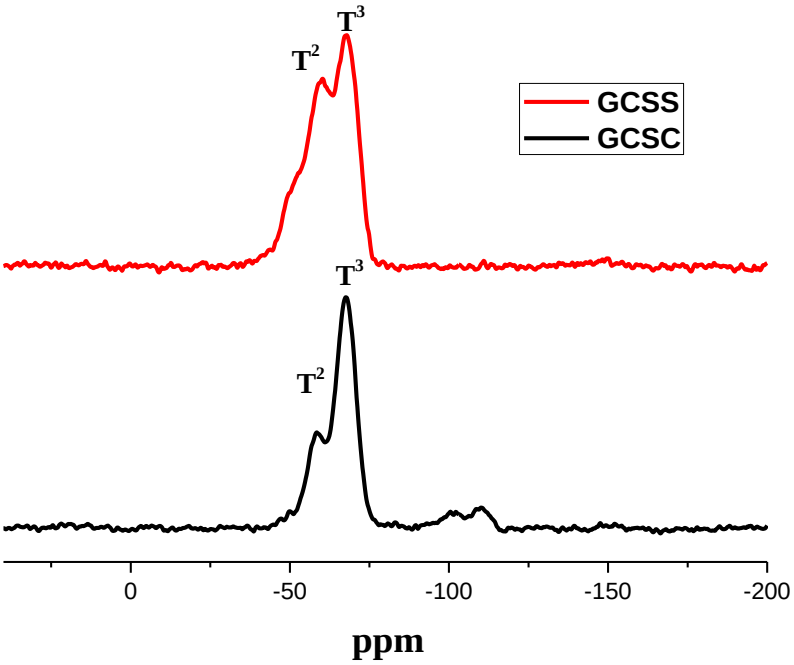

Figure 3: ^{29}Si OP-MAS NMR spectrum of **GCSC** and **GCSS**.

3.3. X-ray diffraction

Figure 4 shows X-ray diffractograms of chitosan and N-guanidinium chitosan acetate **GC** (left), **CGSS-CP** and **CGSC-CP** (right). Neat chitosan shows the typical reflection at 2θ = 20.1° which can be attributed to the crystalline structure of the chitosan chains [10]. In the diffractogram of **GC**, this peak can also be observed. A new diffraction ray at 2θ = 26.2 and other broad rays at 34.9° and 39.1° reflect the formation of a new crystalline structure for the new guanidinium side chains in this latter material. The increase of the crystallinity of chitosan by derivatization, *i.e.* the introduction of new side chains on the chitosan backbone, has already been reported in in literature [27].

The X-ray diffractograms of the mineralized *N*-guanidinium chitosan/silica hybrids **CGSS-CP** and **CGSC-CP** are more complex. They show diffraction peaks which assigned to the nucleated hydroxyapatite. These peaks are centered at 2θ = 31.9°, 39°, 46.7°, and 49.7°, corresponding to (002), (211), (112), (300), and (222) planes of hydroxyapatite, respectively [28]. These results indicate that the nucleated calcium phosphate phases in CGSC and CGSS are constituted of similar crystalline phases and mainly contain hydroxyapatite.

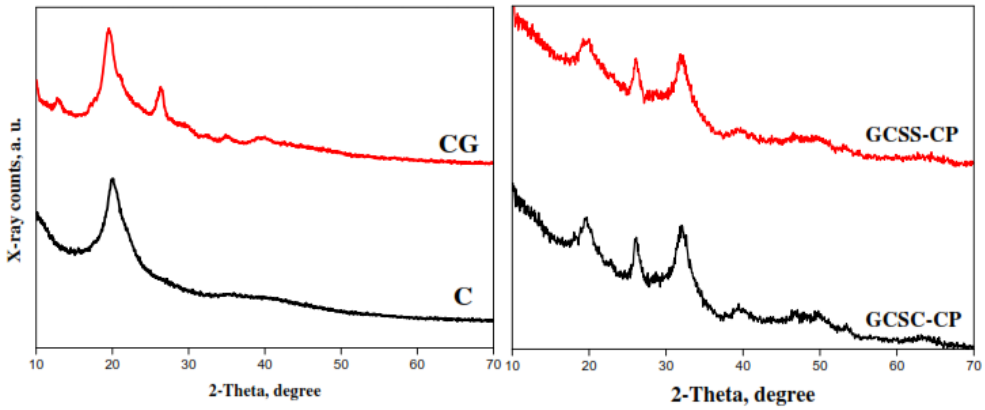

Figure 4: XRD patterns of chitosan (**C**), N-guanidinium chitosan acetate (**GC**), mineralized *N*-guanidinium-chitosan acetate/silica containing sulfonate groups (**GCSS-CP**) and mineralized *N*-guanidinium-chitosan acetate/silica containing carboxylate groups (**GCSC-CP**).

3.4. SEM and EDX

We performed SEM and EDX measurements in order to monitor the morphological and chemical modifications of the materials during the subsequent synthesis steps. Figure 5 shows the SEM images of the prepared materials. N-guanidinium chitosan (GC) shows a relatively homogeneous surface without specific morphology. *N*-guanidinium-chitosan acetate/silica containing sulfonate groups (GCSS) consists of separated particles of flax seeds-like shape with an average diameter of about 500 nm. However, *N*-guanidinium-chitosan acetate/silica containing carboxylate groups (GCSC) showed soft morphology without distinct particle shape that may reflect the hydrogen bond formation between N-guanidinium-chitosan acetate and silica containing carboxylic groups.

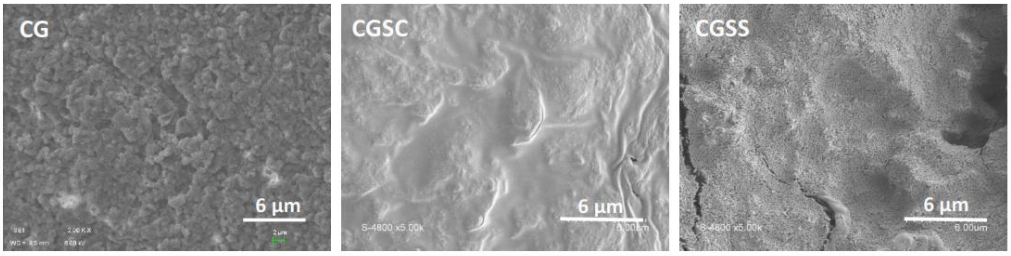

Figure 5: SEM images of *N*-guanidinium-chitosan acetate (**GC**), and the materials **CGSC** and **CGSS**

In addition, SEM analyses were carried out to investigate the effect of anionic groups (carboxylate or sulfonate) in the *N*-guanidinium chitosan acetate/silica hybrids on the morphology of mineralized calcium phosphate. Figure 6 shows SEM images and EDXs spectra of **GCSC-CP** and **GCSS-CP**. SEM images show that the two materials display different morphologies. The mineralized calcium phosphate with carboxylate containing groups (**GCSC-CP**) show a sponge-like morphology with micrometer sized globular aggregates composed of hierarchical nanoplates. The length of these nanoplates is less than 300 nm. On the other side, the material **GCSS-CP**, is composed of calcium phosphate layers and nanospheres without a well-defined morphology. As the mineralization occurred under similar condition in terms of pH and time, these results indicate that nature of the functional ionic group plays an important role in the mineralization process and led to materials with different morphologies and textures. As the intermediate **GCSC** and **GCSS** chitosan/silica

hybrid composites contain a high amount of charged species, strong ionic interactions with both calcium and phosphate ions during the biomineralization process can be assumed. The effect of functional groups of the polymeric materials on the morphology of the mineralized calcium phosphate was already reported in the literature [29]. For example, Mai et al. reported that poly(ethylene oxide) and poly(3-sulfopropyl methacrylate) block copolymers initiate the formation of well-defined hydroxyapatite spheres. The strong effect of this copolymer is probably due to the formation of auto-assembled phases the highly charged block copolymer [30].

SEM combined with energy-dispersive X-ray spectroscopy (EDX) allows mapping of the elements that are forming these structures, as shown in figure 6. EDX spectra show that the **CGSS-CP** and **CGSC-CP** phases contain carbon, oxygen, nitrogen, sodium, silicon, phosphorus, and calcium. The presence of carbon, nitrogen and oxygen is due to the presence of *N*-guanidinium-chitosan acetate. Silicon originates from silica network. The homogenous distribution of silicon suggests true organic/inorganic hybrid nature of the material. The other elements are due to the formation of the calcium phosphate phases. As the mineralization was carried out in SBF, some other elements besides calcium, phosphorus, and oxygen have also been incorporated. EDX thus shows that the grown calcium phosphate is closely related to natural bone in the sense that the apatite contains a variety of elements that are also found in bone such as Na, k and Mg. The Ca/P molar ratios are of 1.48 and 1.44 for **CGSC-CP** and **CGSS-CP**. This value is lower than the theoretical value for pure hydroxyapatite (1.67) [1]. The XRD results and also Ca/P ratio from EDXs measurements suggest that the mineralized calcium phosphate is mainly constituted of hydroxyapatite. However, the deviation of Ca/P ratio from that of pure hydroxyl apatite can be attributed to the formation of additional amorphous calcium phosphate or other crystalline calcium phosphate phases as already reported in the literature [1,31].

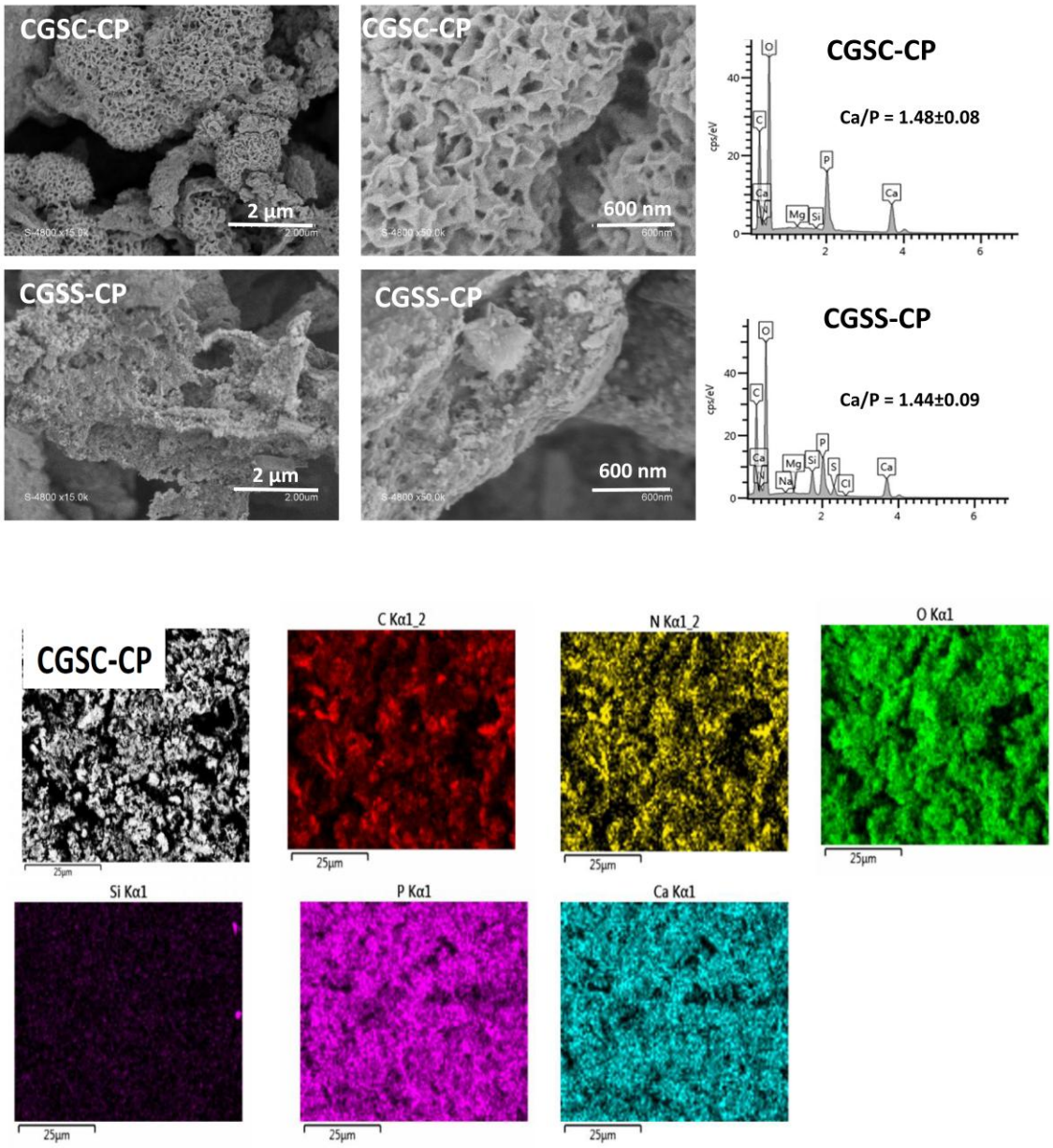

Figure 6: SEM images and EDXs of **GCSC-CP** and **GCSS-CP** and elemental maps for **CGSC-CP**.

3.5. TEM analysis

TEM images of the materials are given in figure 7. These micrographs further confirm the hierarchical structure of the sponge like architecture of **GCSC-CP** which consists of plate-shaped nanoparticles. Precipitation of calcium-phosphate salt preferentially occurred on the carboxylate containing hybrid because carboxylic groups acted as Ca^{2+}-binding site [32]. On the other side, TEM micrographs of **GCSS-CP** showed the

presence of granular-like aggregates that resembled those observed in aqueous solutions.

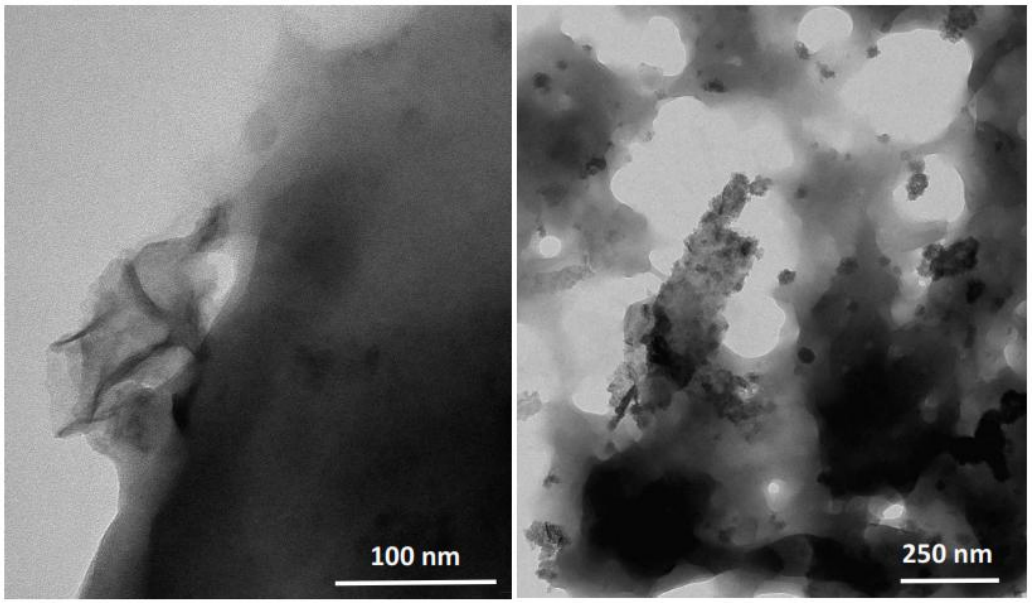

Figure 7: TEM images of **CGSC-CP** (left) and **CGSS-CP** (right)

3.6. Thermogravimetric analyses

It has been reported that silica content increases the thermal stability of chitosan-based hybrids [33]. Figure 8 shows the TGA thermograms of all reported hybrid materials compared between all the hybrids in the term of inorganic content and thermal stability. At a first glance, the residual mass of the **GCSS** and **GCSC** materials is relatively similar (16.2% vs. 17.7%). This result indicates a similar content of anionic silica hybrid material within the two materials. However, after calcium phosphate mineralization, we observed important differences between the two resulting materials **GCSS-CP** and **GCSC-CP**, with residual masses of 29.3 % of the first one and 39.7 % for the second one. These results indicate that the calcium phosphate content of the *N*-guanidinium-chitosan acetate/silica containing carboxylate groups hybrid after 7 days incubation was significantly higher than the one obtained with *N*-guanidinium-chitosan acetate/silica containing sulfonate groups. We attribute these differences to the chemical nature of the intermediate chitosan-silica hybrid composites. It appears that the presence of carboxylate groups in **GCSC** not only affects the morphology of nucleated calcium phosphate, but also resulted in a significant increase of the amount of formed calcium phosphate. The retardation

effect of sulfonate groups in the GCSS may be the reason for this behavior. Indeed, a significant retardation in calcium phosphate precipitation has already been reported using the charged polymers, and this in particular compared to polymer-free conditions [30].

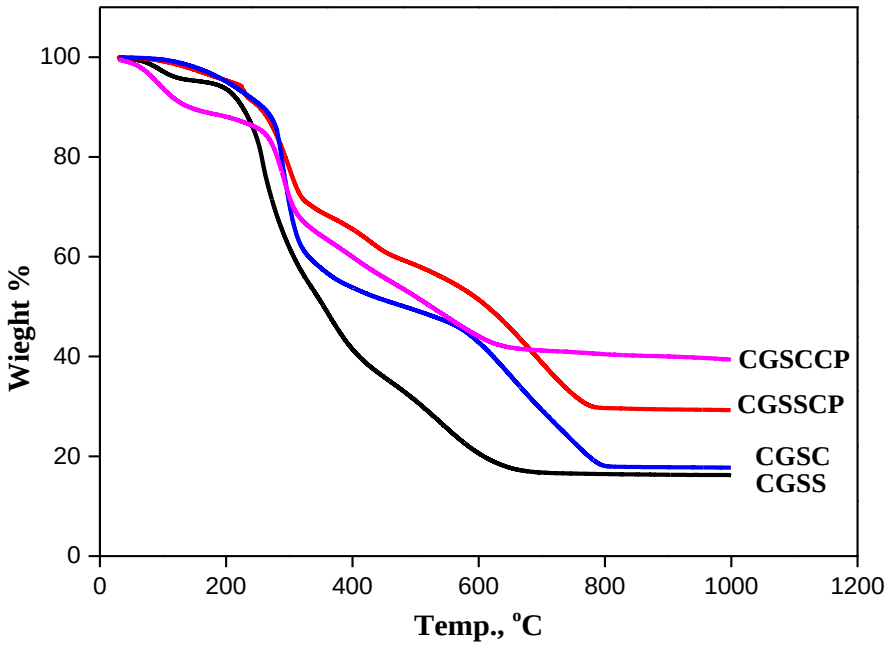

Figure 8: Thermogravimetric analyses of **CGSC**, **CGSS**, **CGSC-CP** and **CGSS-CP**.

4. Conclusion

Novel ionic hybrids were successfully prepared and investigated to enhance the biomimetic mineralization of calcium phosphate. Sulfonate and carboxylate-containing chitosan/silica hybrid composites were synthesized from anionic trialcoxysilylated precursors and *N*-guanidinium-chitosan acetate. The ionic hybrids showed a strong effect on the mineralization of calcium phosphate. The nature of the anionic groups (carboxylate or sulfonate) not only affects the morphology of the formed calcium phosphate, but also resulted in a significant difference of the amount of formed calcium phosphate between the two materials. Our results show that *N*-guanidinium-chitosan acetate/silica hybrid composite containing carboxylate groups is more efficient to induce heterogeneous nucleation and growth of hydroxyapatite. Overall, our data suggest that *N*-guanidinium-chitosan acetate/silica containing

anionic groups are interesting materials for applications in the biomaterials field, in particular for biomineralization processes.

Notes:

The authors declare no competing financial interest

ACKNOWLEDGMENT

This work was financially supported by the Embassy of France in Egypt – Institut Français d'Egypte (IFE) and Science & Technology Development Fund (STDF) in Egypt for the financial support.

References

[1] S. Schweizer, A. Taubert, Polymer-controlled, bio-inspired calcium phosphate mineralization from aqueous solution., Macromol. Biosci. 7 (2007) 1085–99. doi:10.1002/mabi.200600283.

[2] A. Salama, Cellulose/calcium phosphate hybrids: New materials for biomedical and environmental applications, Int. J. Biol. Macromol. 127 (2019) 606–617. doi:10.1016/j.ijbiomac.2019.01.130.

[3] Y. Liu, N. Li, Y.P. Qi, L. Dai, T.E. Bryan, J. Mao, et al., Intrafibrillar collagen mineralization produced by biomimetic hierarchical nanoapatite assembly, Adv. Mater. 23 (2011) 975–980. doi:10.1002/adma.201003882.

[4] C. Hu, L. Zhang, M. Wei, Development of Biomimetic Scaffolds with Both Intrafibrillar and Extrafibrillar Mineralization, ACS Biomater. Sci. Eng. 1 (2015) 669–676. doi:10.1021/acsbiomaterials.5b00088.

[5] T. Ogiwara, A. Katsumura, K. Sugimura, Y. Teramoto, Y. Nishio, Calcium Phosphate Mineralization in Cellulose Derivative/Poly(acrylic acid) Composites Having a Chiral Nematic Mesomorphic Structure, Biomacromolecules. 16 (2015) 3959–3969. doi:10.1021/acs.biomac.5b01295.

[6] A. Salama, Carboxymethyl cellulose-g-poly (acrylic acid)/calcium phosphate composite as a multifunctional hydrogel material, Mater. Lett. 157 (2015). doi:10.1016/j.matlet.2015.05.088.

[7] R.J. Coleman, K.S. Jack, S. Perrier, L. Grøndahl, Hydroxyapatite mineralization in the presence of anionic polymers, Cryst. Growth Des. 13 (2013) 4252–4259. doi:10.1021/cg400447e.

[8] A. Salama, M. Neumann, C. Günter, A. Taubert, Ionic liquid-assisted formation of cellulose/calcium phosphate hybrid materials, Beilstein J. Nanotechnol. 5 (2014) 1553–1568. doi:10.3762/bjnano.5.167.

[9] L.S. Connell, F. Romer, M. Suárez, E.M. Valliant, Z. Zhang, P.D. Lee, et al., Chemical characterisation and fabrication of chitosan–silica hybrid scaffolds with 3-glycidoxypropyl trimethoxysilane, J. Mater. Chem. B. 2 (2014) 668. doi:10.1039/c3tb21507e.

[10] A. Salama, P. Hesemann, Synthesis of N-Guanidinium-Chitosan/Silica Hybrid Composites: Efficient Adsorbents for Anionic Pollutants, J. Polym. Environ. 26 (2018) 1986–1997. doi:10.1007/s10924-017-1093-3.

[11] A. Salama, P. Hesemann, New N-guanidinium chitosan/silica ionic microhybrids as efficient adsorbent for dye removal from waste water, Int. J. Biol. Macromol. 111 (2018) 762–768. doi:10.1016/j.ijbiomac.2018.01.049.

[12] V.K. Thakur, M.K. Thakur, Recent advances in graft copolymerization and applications of chitosan: A Review, (2014).

[13] P.B. Malafaya, R.L. Reis, Bilayered chitosan-based scaffolds for osteochondral tissue engineering: Influence of hydroxyapatite on in vitro cytotoxicity and dynamic bioactivity studies in a specific double-chamber bioreactor, Acta Biomater. 5 (2009) 644–660. doi:10.1016/j.actbio.2008.09.017.

[14] G. Wang, L. Zheng, H. Zhao, J. Miao, C. Sun, H. Liu, et al., Construction of a fluorescent nanostructured chitosan-hydroxyapatite scaffold by nanocrystallon induced biomimetic mineralization and its cell biocompatibility, ACS Appl. Mater. Interfaces. 3 (2011) 1692–1701. doi:10.1021/am2002185.

[15] X. Wang, J. Shi, Z. Li, S. Zhang, H. Wu, Z. Jiang, et al., Facile one-pot preparation of chitosan/calcium pyrophosphate hybrid Micro flowers, ACS Appl. Mater. Interfaces. 6 (2014) 14522–14532. doi:10.1021/am503787h.

[16] B.J. Calnan, B. Tidor, S. Biancalana, D. Hudson, A.D. Frankel, Arginine-mediated RNA recognition: the arginine fork., Science. 252 (1991) 1167–1171. doi:10.1126/science.252.5009.1167.

[17] Y. Hu, Y. Du, J. Yang, J.F. Kennedy, X. Wang, L. Wang, Synthesis, characterization and antibacterial activity of guanidinylated chitosan, Carbohydr. Polym. 67 (2007) 66–72. doi:10.1016/j.carbpol.2006.04.015.

[18] W. Sang, Z. Tang, M. He, Y. Hua, Q. Xu, Synthesis and preservative application of quaternized carboxymethyl chitosan containing guanidine groups, Int. J. Biol. Macromol. 75 (2015) 489–494. doi:10.1016/j.ijbiomac.2015.01.009.

[19] D.Y. Sasaki, K. Kurihara, T. Kunitake, Specific, multiple-point binding of ATP and AMP to a guanidinium-functionalized monolayer, J. Am. Chem. Soc. 113 (1991) 9685–9686. doi:10.1021/ja00025a051.

[20] X. Zhang, Y. Duan, D. Wang, F. Bian, Preparation of arginine modified PEI-conjugated chitosan copolymer for DNA delivery, Carbohydr. Polym. 122 (2015) 53–59. doi:10.1016/j.carbpol.2014.12.054.

[21] M. Iafisco, M. Marchetti, J.G. Morales, M.A. Hernández-Hernández, J.M. García Ruiz, N. Roveri, Silica gel template for calcium phosphates crystallization, Cryst. Growth Des. 9 (2009) 4912–4921. doi:10.1021/cg900702p.

[22] A. Salama, R.E. Abou-Zeid, M. El-Sakhawy, A. El-Gendy, Carboxymethyl cellulose/silica hybrids as templates for calcium phosphate biomimetic mineralization, Int. J. Biol. Macromol. 74 (2015) 155–161. doi:10.1016/j.ijbiomac.2014.11.041.

[23] T. Pirzada, S.A. Arvidson, C.D. Saquing, S.S. Shah, S.A. Khan, Hybrid Carbon Silica Nano fi bers through Sol − Gel Electrospinning, (2014).

[24] S.S. Jedlicka, J.L. Rickus, D.Y. Zemlyanov, Surface analysis by X-ray photoelectron spectroscopy of sol-gel silica modified with covalently bound peptides., J. Phys. Chem. B. 111 (2007) 11850–11857. doi:10.1021/jp0744230.

[25] A. Salama, Chitosan based hydrogel assisted spongelike calcium phosphate mineralization for in-vitro BSA release, Int. J. Biol. Macromol. 108 (2018) 471–476. doi:10.1016/j.ijbiomac.2017.12.035.

[26] Y.-H. Han, A. Taylor, M.D. Mantle, K.M. Knowles, Sol–gel-derived organic–inorganic hybrid materials, J. Non. Cryst. Solids. 353 (2007) 313–320. doi:10.1016/j.jnoncrysol.2006.05.042.

[27] K. Kurita, H. Ikeda, Y. Yoshida, M. Shimojoh, M. Harata, Chemoselective

protection of the amino groups of chitosan by controlled phthaloylation: Facile preparation of a precursor useful for chemical modifications, Biomacromolecules. 3 (2002) 1–4. doi:10.1021/bm0101163.

[28] A. Salama, New sustainable hybrid material as adsorbent for dye removal from aqueous solutions, J. Colloid Interface Sci. 487 (2017) 348–353. doi:10.1016/j.jcis.2016.10.034.

[29] K. Bleek, A. Taubert, New developments in polymer-controlled, bioinspired calcium phosphate mineralization from aqueous solution., Acta Biomater. 9 (2013) 6283–6321. doi:10.1016/j.actbio.2012.12.027.

[30] T. Mai, E. Rakhmatullina, K. Bleek, S. Boye, J. Yuan, A. Völkel, et al., Poly(ethylene oxide) - b - poly(3-sulfopropyl methacrylate) block copolymers for calcium phosphate mineralization and bio film inhibition, Biomacromolecules. 15 (2014) 3901–3914.

[31] A. Salama, M. El-Sakhawy, Regenerated cellulose/wool blend enhanced biomimetic hydroxyapatite mineralization, Int. J. Biol. Macromol. 92 (2016) 920–925. doi:10.1016/j.ijbiomac.2016.07.077.

[32] S. Nardecchia, M.C. Gutiérrez, M.C. Serrano, M. Dentini, A. Barbetta, M.L. Ferrer, et al., In situ precipitation of amorphous calcium phosphate and ciprofloxacin crystals during the formation of chitosan hydrogels and its application for drug delivery purposes., Langmuir. 28 (2012) 15937–46. doi:10.1021/la3033435.

[33] A.Ü. Metin, H. Çiftçi, E. Alver, Efficient removal of acidic dye using low-cost biocomposite beads, Ind. Eng. Chem. Res. 52 (2013) 10569–10581. doi:10.1021/ie400480s.